Tuning, measurement and prediction of the impact of freezing on product morphology: A step toward improved design of freeze-drying cycles

To cite this article:

Roberto Pisano, Andrea Arsiccio, Kyuya Nakagawa & Antonello A. Barresi (2019) Tuning, measurement and prediction of the impact of freezing on product morphology: A step toward improved design of freeze-drying cycles, Drying Technology, 37:5, 579-599,
DOI: 10.1080/07373937.2018.1528451

To link to this article: https://doi.org/10.1080/07373937.2018.1528451

Tuning, measurement and prediction of the impact of freezing on product morphology: a step towards improved design of freeze-drying cycles

Roberto Pisano[1], Andrea Arsiccio[1], Kyuya Nakagawa[2], Antonello A. Barresi[1,*]

[1] Department of Applied Science and Technology, Politecnico di Torino
[2] Division of Food Science and Biotechnology, Graduate School of Agriculture, Kyoto University

[*] Corresponding Author
E-mail: antonello.barresi@polito.it

Abstract
The control of freezing is crucial as it can influence the freeze-drying operation as well as influence the chemical and physical properties of the lyophilized product such as the specific surface area, dissolution rate and drug stability. In this review article, we focus on two areas related to lyophilization in the pharmaceutical industry: (1) advances in our understanding of the relationship between the freezing conditions, product morphology and drying efficiency, and (2) the control of nucleation in solutions to be frozen. The final objective is to accelerate the transition towards a more robust design of freeze-drying cycles, based on deep knowledge of the phenomena involved rather than on empirical observations. While these topics are not new, they are areas of significant current interest to the community engaged in drying in the pharmaceutical industry.

Keywords
Crystal sizing, Freeze-drying, Freezing, Mathematical modelling, Controlled Nucleation

Introduction

Freeze-drying is a process widely used in the pharmaceutical industry. It consists of three steps, namely, freezing, primary drying, and secondary drying. During freezing, temperature is lowered, and the product is frozen. Then, ice and bound water are removed in the subsequent drying phases, by sublimation and desorption, respectively. During primary and secondary drying, the removal of water occurs at low temperatures as a result of the very low pressures involved. Because of this, freeze drying is particularly suitable for the preservation of pharmaceuticals and biopharmaceuticals, which often lose their therapeutic activity at high temperatures.

Freezing is crucial as it can influence the ice crystal size, and thus the product behavior, during drying, as well as other physical properties of the lyophilized product [1-6]. The product morphology is substantially determined by the cooling rate and nucleation temperature. For instance, a low cooling rate and/or a high nucleation temperature promotes the formation of large ice crystals. In this regard, the influence of the nucleation temperature on the pore size is thoroughly discussed in [7]. Freezing conditions can also influence the development of various polymorphic forms for the crystallizing excipients such as mannitol and glycine. This phenomenon is crucial in the pharmaceutical industry as different polymorphs can exhibit different physical and chemical properties and, hence, affect the stability of the drug substance during storage [8, 9]. The various polymorphic forms of a material can show different thermodynamic stability. For example, the α and δ polymorphic forms of mannitol are metastable, while the β form is stable [10]. At the end of the freeze-drying process, the active pharmaceutical ingredients (APIs) will be immobilized within a matrix formed by the excipients, which should be stable with time. In fact, changes in the properties of this matrix during storage could be detrimental to the stability of the APIs. Therefore, formation of a stable polymorphic form is desired as this provides the best conditions for long term storage of the product. A second, not negligible, aspect related to the content of polymorphs is the vial breaking phenomenon. It is thought that vial breaking should be linked to the formation, during freezing, of metastable forms, which then convert into stable ones and cause vial breaking [11, 12]. It is thus obvious that, by controlling the freezing conditions, it would be possible to control and prevent the vial breaking phenomenon.

The morphology of the frozen product has also a strong impact on the rate of the subsequent drying phases. In fact, provided that no shrinkage or collapse occurs, the size of the ice crystals formed during

freezing corresponds to the size of the pores within the dried product. This pore size, in turn, influences both the sublimation and desorption rates [5, 9, 13, 14]. In fact, a large pore size speeds up the removal of water by sublimation but is detrimental to the rate of desorption (see Table 1). Consequently, primary drying benefits from a large pore size, while secondary drying is penalized. Moreover, the pore size influences the maximum temperature reached by the product as well, with higher temperatures reached in the case of smaller pores. Control of the maximum temperature reached by the product is of utmost importance for the freeze-drying process. In fact, if the maximum temperature overcomes a limit value, which is specific for each formulation, collapse of the cake is observed. A collapsed cake loses its aesthetic properties and is generally characterized by a higher residual moisture content, which could damage the active ingredients. The impact of pore size on drying time and maximum temperature reached within the product during primary drying is summarized in Figure 1.

Finally, the dimension of the ice crystals formed during freezing affects the stability of APIs. A major contribution to loss of therapeutic activity is related to adsorption at the ice-freeze concentrate interface [15]. Thus, the larger this interface is, the higher the risk of activity loss is. In this regard, the formation of large ice crystals, achievable by means of a low cooling rate and/or a high nucleation temperature, is desired, since in this case the specific surface area is minimized.

In this work, the various techniques developed for the control of the freezing process of pharmaceutical solutions are described and their impact on the product structure is discussed for two of these technologies, i.e., the ultrasound-induced ice nucleation and the vacuum induced surface freezing, on which we have direct expertise, and which are not currently covered by patents. Finally, the applicability of all the different proposed methods to production plants, with respective advantages and limitations, are analyzed. The possibility to measure the impact of freezing on the product morphology, using in-line and off-line approaches, is also discussed. The in-line method provides a more direct estimation of the information required, i.e., the resistance to mass transfer, but presents several drawbacks. Therefore, other off-line approaches were and are being developed, which employed experimental techniques (BET, SEM, optical microscopy) often coupled with image analysis approaches (2D-Fast Fourier Transform, wavelet compression, image segmentation etc.). Some of these techniques are briefly described. Additionally, the problem of prediction of the product morphology by means of a mathematical model is also discussed. These

models can be used to obtain a quantitative estimation of the influence of the freezing conditions on the average size of ice crystals. It is also discussed how these tools can be applied to tune, measure and predict the impact of freezing on product morphology, and, consequently, on process efficiency and product quality. The aim of this review is to encourage a more knowledge-driven approach to the design of a robust freeze-drying cycle. This would be extremely beneficial, allowing a better control of the homogeneity and quality of the final products.

Control of freezing

While most of the conventional freezing protocols allow control of the cooling rate, the nucleation temperature remains a stochastic variable, randomly distributed within the batch. Because of this, a large vial-to-vial and batch-to-batch variability is observed, and this inhomogeneity contrasts with the stringent requirements of the pharmaceutical industry in terms of process control and product quality. To overcome this problem, various techniques have been developed over the years to promote the control of the nucleation temperature [6, 16, 17]. Among these, vacuum induced surface freezing (VISF) [9, 13, 18-20] and the ultrasound-induced ice nucleation (UIIN, Figure 2a) [21-25] will be considered in detail in the following.

Ultrasounds are acoustic waves with frequencies approximately over 20 kHz. Ultrasound ranging from 20 to 100 kHz is classified as power ultrasound and may be used in chemical and physical applications as it induces the formation of cavitation bubbles [21-25]. These collapsing bubbles and the resulting micro-streaming enhance the mass and heat transfer, affecting the ice nucleation phenomenon, as well. A possible mechanism elucidated by Hickling [26] is that the pressure increment due to the collapse of the cavitation bubble increases the equilibrium freezing temperature of the solution; this phenomenon simultaneously increases the degree of the supercooling. The degree of supercooling is a major driving force of ice nucleation, as it enhances the number of nuclei. Saclier et al. [27] proposed a theoretical model of ice nucleation induced by acoustic cavitation based of the theory of Hickling, and successfully elucidated the relationship between the number of nuclei and the liquid temperature. This theoretical study concluded that the power ultrasound could trigger ice nucleation in a water with a supercooling level higher than a few kelvin using a moderated acoustic pressure amplitude, that is, about one bar. Then, the number of nuclei can

be further increased by lowering the temperature or increasing the acoustic pressure. This theoretical background can well explain experimental findings reported in the literature [28-32].

For instance, Nakagawa *et al*. [32] froze and then freeze-dried mannitol solutions to clarify the detailed relationship between the ice nucleation temperature and the primary drying rate. They found that the primary drying rate increased with increasing ice nucleation temperatures, and the observed dependence on the ice nucleation temperature was similar for both the spontaneously nucleated and the sonically triggered system [32-34]. They also reported that the ice morphology was not greatly affected by the ultrasound trigger, but it was significantly influenced by thermal phenomena (i.e. cooling rate, initial temperature distribution, sample geometry, etc.) [35]. For instance, the increase in cooling rate led to a smaller ice crystal size, and the effect of cooling rate was more important at high nucleation temperatures.

What makes ultrasound interesting is the possibility of application without contact, which makes this technique chemically non-invasive. Some concerns still exist, because localized high temperatures generated by cavitation, and the bubble themselves, can potentially damage or favor aggregation of very sensitive products. Tests carried out in a pilot scale freeze-dryer demonstrated that this technology significantly improves the whole batch homogeneity, without modifying the protein or virus activity. On the contrary, the enzyme activity recovery is higher, as a consequence of the higher nucleation temperature and, therefore, larger ice crystal size (and, thus, smaller ice-freeze concentrate interface). Liquid formulations of Human Recombinant Interferon-A2b have also been tested to verify that the ultrasounds do not promote the aggregation of API molecules [34, 36, 37].

Finally, it can be mentioned that even if transient cavitation is generally employed, it has been evidenced that the ultrasonic vibrations can induce nucleation even in the stable cavitation regime, characterized by bubbles that exhibit stable volume or shape, thus reducing the risk of product denaturation; however, this phenomenon has not been explained yet [38].

In Vacuum Induced Surface Freezing, by contrast, pressure is lowered within the dryer chamber during freezing. This pressure drop promotes ice nucleation as a result of a partial evaporation of water, and, hence, a reduction in the product temperature. Figure 2b shows an example of temperature and pressure profiles observed during a VISF cycle. While the original method described by Kramer et al. [18] and Liu et al. [19] resulted in the formation of defects within the cake structure, such as blow-up and flake formation, the

modifications to the VISF protocols proposed by Oddone et al. [20] allowed the solution of these problems and the production of an elegant cake. As shown in Figure 3, SEM analysis confirmed that VISF promoted the formation of larger pores (Fig. 3b) with respect to uncontrolled nucleation (Fig. 3a). Moreover, a reduced within-vial heterogeneity was observed upon application of controlled nucleation. A similar result was obtained in the case of control of nucleation via UIIN (see Figure 3c, where the ice crystals are shown as observed by optical microscopy just after freezing). Also in this case, nucleation was triggered at a higher temperature, promoting the formation of large pores and enhancing the uniformity of the lyophilized cake. It must be remarked that uncontrolled freezing was carried out in no-GMP conditions and thus nucleation naturally occurred at relatively high temperature, approx. −10 °C, which is not far from that observed in the UIIN freezing. Because of that, the average pore size of samples produced via UIIN was larger, but comparable, to that observed for the uncontrolled samples. The increased, and more uniform, pore dimension had a strong impact on the subsequent drying phase, as well. For instance, Oddone et al. [9, 13, 20] showed that the new VISF approach allowed significant reduction of primary drying times, and a remarkably increase in batch uniformity. Moreover, even if secondary drying of the VISF cycle is usually longer than that of the conventional freezing run, the total cycle time is shorter [13]. Ultimately, a further advantage of VISF is that it does not require installation of additional equipment and can be carried out in any common freeze-dryer, as will be further discussed in the following.

Both these techniques allow a precise control of the nucleation temperature, and result in improved process efficiency and batch homogeneity. Another method which has been proposed is the so-called electrofreezing [39, 40], which uses a high voltage pulse to initiate nucleation in supercooled water. However, the influence of electrofreezing on bubble formation [39], and the inhibitory effect observed in the case of a high saline concentration [40] need further investigation. An alternative solution (which may be applicable only in laboratory studies) may consist in the addition of impurities to the sample being frozen. These impurities, which often consist of silver iodide and bacteria such as *Pseudomonas syringae*, may serve as nucleating agents [5, 19, 41-43], and can help increase the nucleation temperature.

Another freezing protocol which has been investigated in the literature is the high-pressure-shift or depressurization method [44, 45]. According to this technique, the drying chamber is first pressurized to 1.5–4.5 bar, and then rapidly depressurized. This initiates nucleation in the samples, previously equilibrated

at a temperature below the equilibrium freezing point. The application of this approach, however, requires that the freeze-dryer can manage the 0.5–3.5 bar overpressure which is required to trigger the freezing process.

Finally, in the case of the ice-fog technique [46-51], small ice particles, generated by the release of cold nitrogen within the freezing chamber, penetrate into the vials, thus inducing ice nucleation. This ice fog could also be generated within an external condenser, or, alternatively, a gas flow cooled down within the condenser could be used to generate the ice particles inside the drying chamber. However, in the case of the ice fog technique, it is not clear if it can be guaranteed that very big batches of vials, like those used in manufacturing, may be reached by the ice particles, assuring a uniform batch behavior.

All the mentioned approaches for the control of nucleation, such as VISF, UIIN, the depressurization method and the ice-fog technique, act by inducing nucleation at the desired temperature. However, while VISF, the depressurization method and the ice-fog technique trigger nucleation at the surface of the solution and induce a directional solidification, UIIN acts on the bulk product, promoting a global supercooling [6].

Further details on these methodologies can be found in [17] and in references quoted therein, and a more extensive description of their implementation in industrial plants will be provided in the following.

Prediction and measurement of the impact of freezing on product morphology

Starting from this premise, it is clear that the measurement and prediction of the impact of freezing on product morphology plays a central role in the design of a robust freeze-drying cycle. The most important parameters related to product morphology are the pore diameter D_p, and the tortuosity τ. When modelling the freeze-drying process, the desired input value of D_p would be the diameter of equivalent mass transfer resistance, i.e., the diameter leading to the experimental value of product resistance. However, a standard procedure for the experimental evaluation of the diameter of equivalent mass transfer resistance has not yet been defined, and its definition would be trivial only for tubular pores of uniform dimension. In real situations, pores do not have a perfect tubular structure, and do not share the same dimension. Therefore, some approximations must be done when defining an average D_p for the dried cake, and these approximations depend on the available data and on the approach used for their analysis. For instance, in the case of 2D images of a porous structure, the pore section is sometimes approximated with an ellipse, and the

diameter of the circle having the same area to perimeter ratio of the approximating ellipse may be chosen as pore diameter. SEM images can be analyzed in this way, considering a sufficiently large number of pores and taking the numerical average of this distribution as an approximation for D_p. Otherwise, the total area occupied by the pores in the 2D image could be calculated and divided by the number of pores. In this way, an average sectional area for the pores is calculated, and the diameter of the circle having this area is assumed as D_p. In the case of 3D reconstructions, such as for micro-computed tomography, either the number-weighted or volume-weighted distribution of the pore sizes can be usually obtained, and the average of these distributions can be used. If an indirect information about the pore size is obtained, as in the case of the specific surface area provided by BET, a model can be used to link the surface area to the pore size. A more detailed description of the possible approaches for estimation of D_p or τ is provided in the following.

From D_p and τ it is possible to calculate the mass transfer resistance to vapor flow during primary drying, R_p, which is an essential input for any model of primary drying. During primary drying, a very low pressure is used, and the solvent vapor is removed through the small pores which are formed in the dried product. Because of this, the mass transfer generally occurs in the free-molecule or Knudsen regime. This is the assumption that is generally made when modelling the lyophilization process. An accurate description of the mass transfer is therefore essential for modeling the lyophilization process. In fact, whereas at the beginning of primary drying the heat transfer controls the sublimation kinetics, the mass transfer may become the controlling mechanism towards the end [52, 53]. Moreover, it was also shown that the controlling mechanism may vary according to product morphology and process conditions, such as the shelf temperature and the chamber pressure [53]. In this context, if the porous cake is assumed to be a collection of capillary tubes, the dried layer resistance R_p as function of the dried layer thickness L_d can be calculated as [47]:

$$R_p = \frac{3\tau^2 L_d}{2\varepsilon D_p}\sqrt{\frac{\pi \mathrm{R} T}{2M_\mathrm{w}}} \tag{1}$$

where R is the universal gas constant, T the absolute vapor temperature which can be taken equal to the interface temperature of the frozen product, M_w the molar mass of water, and ε the porosity. There are also other experimental methods which can directly measure R_p, thus overcoming the necessity to know D_p and τ. These approaches, which are often based on the measurements of sublimation rate and product temperature, have, however, several drawbacks. First of all, a labor-intensive procedure is needed, which requires the

execution of several experimental tests [54-58]. In fact, a preliminary estimation of the actual heat transfer coefficient k_v between the container and the shelf must be first carried out. This can be achieved by measuring the product temperature (T_p) profile as function of time, using, for instance, miniaturized thermocouples. The temperature evolution of the heat transfer fluid circulating through the drier shelves (T_f) should also be known. The vapor flow rate (J_w) produced by ice sublimation can then be estimated thanks to the heat transfer coefficient k_v, e.g., assuming that all of the heat transferred to the product is used for the phase change,

$$J_w = \frac{k_v \left(T_f - T_p \right)}{\Delta H_s} \tag{2}$$

where ΔH_s is the enthalpy of sublimation.

From the product temperature profile, it is also possible to calculate the vapor pressure of ice $p_{w,i}$ [59], while the chamber pressure, p_c, can be measured, for instance, by means of a capacitance manometer (i.e., Baratron). When all these variables are known, it is then possible to obtain R_p from the following equation,

$$J_w = \frac{1}{R_p} \left(p_{w,i} - p_c \right) \tag{3}$$

However, a major drawback of these approaches is related to the presence of the miniaturized thermocouples, which may alter the drying process, thus affecting the quality of the estimations. Moreover, this method is generally limited to lab pilot plants, since the use of thermocouples is not compatible with GMP procedures. While the methods based on thermocouple readings refer to individual vials, there are other methods proposed in the literature which estimate the average state of a group of vials or of the entire batch. To provide an example, a micro-balance can monitor both mass and temperature of a limited number of vials during the entire cycle [60]; as an alternative, the Pressure Rise Test (PRT) can be used to estimate temperature, residual moisture, heat and mass transfer parameters during both primary [61-69] and secondary drying [70]. The PRT is based on the analysis of the process response to a step change in input. More specifically, the valve between the vacuum chamber and the condenser is closed for a certain time interval (short during primary drying, longer during secondary drying). Therefore, the pressure inside the chamber increases, because of the accumulation of water vapor. At the beginning, the increase in pressure is fast, but then it proceeds more slowly when the chamber pressure approaches the equilibrium value. If the pressure

profile inside the vacuum chamber is collected during the PRT, it is subsequently possible to obtain useful information about the process, such as the temperature at the sublimation interface and the sublimation flow rate. Moreover, also other parameters, such as the heat transfer coefficient k_v between the shelf and the vials, and the mass transfer resistance to vapor flow R_p, can be estimated from the PRT. Several model-based methods have, therefore, been developed for monitoring primary drying using the PRT, i.e. the Manometric Temperature Measurement [62-64], the Pressure Rise Analysis [65], and the Dynamic Parameters Estimation [66-67].

However, a limitation of these solutions is that they are often ill-conditioned [68]. This means that small variations in inputs cause very large variations in the estimated value of the resistance to mass transfer. Considering the unavoidable uncertainty on measurement of the input quantities, these approaches are thus not compatible with an industrial process. To solve this problem, a modification of the Dynamic Parameters Estimation algorithm was proposed in order to improve problem conditioning, and, thus, the accuracy of the estimation [68].

It is well known that a batch of vials can exhibit a significant degree of heterogeneity. This is due to the different nucleation temperature of the vials in the batch, and to the different position of the vials within the chamber, which affects, for instance, their exposure to radiant heat. It is also evident that this vial-to-vial heterogeneity can dramatically affect process efficiency and product quality. However, the PRT-based techniques cannot explicitly account for the inter-vial variability. In fact, these approaches basically assume that all the vials of the batch behave in the same way, and their state corresponds to the state of the batch as a whole. To address this problem, Velardi et al. [66], Velardi and Barresi [67] and Barresi et al. [69] introduced a correction coefficient to account for the inter-vial heterogeneity within the dynamic parameters estimation algorithm.

Also methods based on the measurement of the temperature profile in the vial generally sample a single vial taken as representative of the whole batch, even if in principle several vials can be monitored (but with the limitations described before).

As an alternative to these techniques there are other approaches, such as BET, SEM, microscopy, and X-ray micro-computed tomography, which provide the value of mass transfer resistance for the single vial under investigation. In this case, the “average batch value” is unknown, and can only be deduced from a

significant number of “local values” for the single vials. Moreover, analysis of the single vial allows estimation of the intra-vial variability in pore size. This within-vial heterogeneity may also significantly affect the calculation of the mass transfer resistance. In fact, if the average pore dimension is introduced into Equation 1, the value of R_p which is computed cannot be accurate, especially if the dried sample is highly heterogeneous. If, however, the whole distribution of pore size within the product height is known, it is possible to divide the sample height into horizontal layers, calculate a different value of $R_{p,i}$ for each layer, and then compute the overall mass transfer resistance as $R_p = \sum_i R_{p,i}$. This approach gives a more accurate description of the dependence of R_p on the thickness of the dried layer, mainly when this relationship is non-linear.

Another common feature of these alternative approaches for estimation of the mass transfer coefficient, such as BET and SEM, is that they can be used off-line, and do not require the placement of any sensor inside the freeze-dryer. In fact, all these approaches are based on indirect calculation of the mass transfer coefficient, based on the cake structure and porosity.

For instance, BET may be employed to measure the specific surface area of the freeze-dried samples [47]. The specific surface area of the freeze-dried cake is related to the pore size, which in turn corresponds to the size and morphology of the ice crystals. In fact, assuming that the pores are cylinders with diameter D_p and length l_{eff}, the specific surface area SSA of the pores may be expressed as

$$SSA = \frac{n\pi D_p l_{eff}}{\rho_s V_s} \tag{4}$$

where n is the total number of pores in the solid having density ρ_s and volume V_s. Thus, BET analysis could be used to obtain indirect information on product morphology, which could then allow calculation of the mass transfer coefficient R_p. A problem connected with this type of analysis, however, is that the specific surface area is influenced by a number of factors, other than pore dimension. For example, when measuring specific surface area, the morphological habit and surface roughness of the sample come into play as well, and their effect cannot be decoupled from pore dimension.

Another possible approach makes use of SEM analysis, generally performed at different positions along the vertical section of the cake. After obtaining the SEM images, several techniques may be applied on them to ease the subsequent analysis. For instance, regulation of contrast and brightness, smoothing by application

of filters, and, finally, the choice of an appropriate threshold for the identification of pores should be taken into account (details can be found in [71]). Then, image analysis techniques could be used to derive the pore size distribution from the processed images. Several commercial image analysis tools exist, such as, for example, *ImageJ*, but, according to the authors' experience, results provided by these tools are not completely reliable. In fact, SEM images cannot be easily processed using these tools, because of the difficulty to clearly detect pore edges. Thus, the result is that the process cannot be automatized, and results obtained strongly depend on the operator who performs the analysis. To address this problem, a number of ad hoc image analysis approaches have been proposed over the years. For instance, a technique based on frequency domain processing was described in 2016 [71]. More specifically, two possible solutions were developed, which were based on 2D Fast Fourier Transform (2D-FFT) and on wavelets compression, respectively [72-73].

Using 2D-FFT [72], an estimation of the brightness spatial frequency distribution could be obtained, which is in turn related to the pore size distribution. That is, SEM images with larger pores will have their energy concentrated at low frequencies, while images with smaller pores will have an energy which spreads over a larger spatial frequency range.

In the case of wavelet compression [73], SEM images were compressed filtering out high frequency spatial components. Since wavelet compression filters out part of the frequencies, the image energy decreases during the process. Following the energy reduction due to the compression can be a way to obtain information on the pore size distribution.

A relationship exists between the pore size distribution (or average pore size) and the mass transfer coefficient (or the cake resistance), as shown in Eq. (1), even if tortuosity has a relevant impact. In fact, if one considers the pores to be straight and tubular, a linear relationship can be easily found between the pore area and the mass transfer coefficient. But experimental results confirm that a linear relationship is also applicable to real cake structures as shown in [72]. Alternatively, an Artificial Neural Network trained to estimate the mass transfer coefficient may be employed. This approach was tested in Ref. [73], after wavelet compression; the training data were obtained through the Pressure Rise Test technique, but can potentially be generated by other methodologies that can provide an estimation of the effective diffusivity to mass transfer.

The accuracy of the Artificial Neural Network estimations is directly correlated to the size and accuracy of the training data set.

Actually the techniques based on 2D-FFT and wavelet compression were tested upon nine formulations, using both crystallizing and amorphous excipients, at different concentrations, up to 10%. It was found that both 2D-FFT and wavelet gave results comparable with the values obtained by the PRT, with the only exception of formulations having highly interconnected pores, for which the mass transfer coefficient was underestimated.

Recently, an image analysis approach based on image segmentation has been proposed [74]. In this case, the SEM image was partitioned into multiple sets of pixels, defined as super-pixels, sharing certain characteristics. The area (in pixels) that each super-pixel covered could then be easily calculated. If each pore within the SEM image was identified as a separate super-pixel, the pore size distribution could therefore be easily evaluated, first in pixels, and then, using the scale of the SEM image, in μm. This image segmentation approach was tested upon different formulations, containing both crystalline and amorphous solutes, and different concentrations. In any case, results obtained were proven to be in accordance with other more traditional approaches to image analysis. However, a not negligible advantage of the segmentation approach was that it allowed a much faster, and potentially automatable, analysis.

Another experimental technique, other than BET and SEM, which could be used, is the X-ray micro-computed tomography [75]. In this case, the entire porous internal structure of the lyophilized samples can be reconstructed. Based on this reconstruction, it is then possible to obtain the pore size distribution within the product, and, then, the resistance to mass transfer. In the work by Pisano et al. [75], the reconstructed structure was partitioned into 10 cylindrical disks and each disk was post-processed using SkyScan CT-analyzer program to estimate its porosity. This pore size distribution was then converted into the mass transfer resistance coefficient. Using this approach, a good agreement was obtained with experimental values of the mass transfer resistance obtained by the pressure rise test method, for both conventional freezing and VISF. The calculation of the resistance to vapor flow requires that the tortuosity is known. Theoretically, this parameter could be estimated from the ratio of open pore length to the length of the sample. However, it is practically impossible to obtain an accurate estimation of the pore interconnectivity, because of the low resolution of the X-ray micro-computed tomography with respect to the thickness of the pore wall.

Therefore, all the approaches described so far can only derive information on the pore size, while no information is obtained for the tortuosity value τ. Thus, a value for τ based on theoretical considerations, or fitting of experimental data, is generally used for calculation of the resistance to mass transfer R_p, as discussed before.

Tortuosity values reported in previous studies [76-80] typically ranged between 1.2 and 3.8. By contrast, Goshima et al. [81] proposed a solution which could provide estimation of both D_p and τ, starting from microscopic observation of frozen samples. They used a series of 2D images obtained at different depth to reconstruct the 3D structure, which was then digitally sliced in the other two orthogonal planes to estimate the path length and the effective pore length (see Figure 4). In this case, the tortuosity is defined as the ratio of the path length (L) to the distance between the origin and the end (L_0).

$$\tau = L / L_0 \tag{5}$$

Considering an ideal cylindrical pore of length l_{eff} and diameter D_p that is inclined from the vertical axis by an angle φ, the tortuosity can be written as,

$$\begin{cases} 1/\tau = 1 & 0 \le \varphi < \theta \\ 1/\tau = \cos(\varphi - \theta) & \theta \le \varphi < \pi \end{cases} \tag{6}$$

where θ is the diagonal angle of the rectangular pore cross section,

$$\theta = \arctan\left(D_p / l_{eff} \right) \tag{7}$$

Image analyses carried out by Goshima et al. [81], in order to obtain the values of φ, D_p and l_{eff}, and, therefore, of τ, on the optical images of frozen solutions showed that the ice microstructure was constituted by flat-shaped ice crystals with roughly oval cross section (with random orientation in the case of conventional freezing). They obtained mean tortuosity values in the range 2.9 to 3.2, for a formulation composed of sucrose and BSA. The impact of the tortuosity on primary drying was also estimated in [81], predicting that a decrease in the tortuosity from 3.5 to 1.5 significantly enlarges the design space of the freeze-drying process. That is, the reduction in tortuosity and the increase in mean ice crystal size were found to have a similar impact.

The method described above is very labor-intensive, thus alternative methods to estimate τ or characterize the pore structure would be advisable. For instance, a procedure to estimate, using computational fluid

dynamics, the tortuosity of a cake reconstructed by randomly assembling pores of appropriate size as indicated by 2D SEM images, has been recently proposed by the authors, and is currently under development [82].

Also the freeze-drying microscope (FDM) can be a useful tool in this context. However, while FDM may be very valuable to evaluate the influence of the cake structure on the lyophilization kinetics, as shown by Raman [83] and by Ray et al. [84], in the opinion of the authors it is very difficult to predict or reproduce via FDM the actual structure obtained in vials used in the industrial apparatus [85]. The use of FDM has been proposed by Pikal et al. mainly for studying the morphology of the crystal/pore structure obtained from different freezing and annealing regimes [86]; later on, Kochs et al. [85, 87] pursued its use for kinetic studies, and the technique was further developed by Ray et al. [84]. The use of the FDM offers some advantages in this respect; it allows an easy estimation of the effective diffusion coefficient D_{eff} , which describes the diffusion of water vapor from the inner frozen core through the outer dried cake of the sample being freeze dried, and can be determined from the relationship between the thickness of the dried cake and the sublimation time. Since FDM allows the direct observation of the movement of the sublimation front, the value of D_{eff} can be efficiently estimated by this technique [88]. An advantage of this approach is that values of D_{eff} were found to be constant at temperatures below the collapse temperatures of the dried cakes, while R_p lumps the cake temperature and structure, and thus it is expected to depend (even if not strongly) on product temperature. Moreover, in FDM both one-dimensional planar and cylindrical geometries can be studied, which simplifies analysis. On the other hand, this planar structure may be very different from the one obtained in the freeze-dryer. In addition, during the cooling step in the FDM, nucleation of the sample can neither be controlled nor predicted, and results are poorly reproducible [89], unless an ice nucleator like AgI is used [84].

Along with experiment-based approaches, model-based techniques exist as well, which allow prediction of pore size distribution and, thus, of the mass transfer resistance within the product being dried. While several mechanistic models for primary drying have been developed over the years, the literature on models for the freezing process is not as extended. Two models of the freezing process were developed by Nakagawa et al. [90] and Pisano and Capozzi [91], for shelf-ramped freezing and VISF respectively. Starting from input data such as cooling rate, heat transfer coefficients and nucleation temperature, these models

allow prediction of the whole temperature profiles within the product being frozen. These temperature profiles may then be used to obtain the freezing front velocity and temperature gradients within the already frozen zone, that are the required data for calculation of the pore size distribution. For performing this calculation, both empirical laws [92-94], and a recently developed mechanistic model [95], exist. Both these approaches allow estimation of the intra-vial pore-size variability, that significantly affects the calculation of the mass transfer resistance.

However, while empirical laws are simply based on fitting of experimental data, the mechanistic model for ice crystal size prediction is based on mass and energy balance equations, which can provide insight into process phenomena, and was developed in both a detailed and a simplified version. In its first formulation, this mechanistic model still contained a term which could not be accessed experimentally and had to be calculated from fitting of experimental data. This term accounted for the free energy change due to the generation of a new ice-freeze concentrate interface. Recently, we found that this term could be approximated using Molecular Dynamics simulations [96]. In fact, upon simulation of a box undergoing a freezing process, it is possible to calculate the decrease in energy due to the formation of ice. We observed that, in the case of pure water, the energy change per frozen molecule was larger than the same value measured, for instance, in the case of a 5% w/w mannitol or sucrose solution. The smaller energy change per molecule in the case of the freezing of water-sugar solutions could be explained assuming that a new ice-freeze concentrate interface had to be generated, and this interface generation required energy to be completed. Therefore, the analysis of the difference in energy change upon freezing could be used to estimate the free energy change due to the generation of new interfaces. A more detailed description of this approach can be found in [96], where the model described in [90, 91] was used to obtain the design space for the freezing process.

In Figure 5, an example of application of the previously described models for pore size prediction is shown. The figure displays the pore dimension as function of the vertical coordinate z (setting $z = 0$ at the product bottom) in the case of samples obtained by either uncontrolled freezing or VISF. As expected the average pore size, defined as the numerical average of the pores diameter predicted by the model or measured by SEM analysis, was much larger for VISF than for uncontrolled freezing. This result can be

explained considering that VISF triggered nucleation at much higher temperature than uncontrolled freezing, –5 °C vs. –10÷–15 °C.

Considering that the sublimation process occurs through the pores of the dried product, pore network models could provide further insight into this phenomenon [97, 98]. Pore network models are based on direct simulations of fluid flow in the pores. First of all, a virtual representation of the porous medium is created. Afterwards, the fluid flow through this medium is simulated.

Simulations using pore network models are much less computationally demanding than particle-based methods and have been widely used for describing transport phenomena in porous media [99-102]. However, for application of this technique to the lyophilization process, the equations describing gas flow in the Knudsen regime should be incorporated into the model.

Therefore, it is our opinion that the previously described tools should be combined, in order to guarantee optimal design of freeze-drying cycles. For instance, a possible approach to the choice of suitable freezing conditions is shown in Figure 6. First of all, some initial tests should be performed to gain the required information on the system under investigation. The product morphology could then be predicted using a model, for all possible values of operating conditions. This knowledge of product morphology could then be coupled with a model for primary drying and used to calculate the freezing conditions that maximize process efficiency, preventing collapse or shrinkage of the cake as well.

We are convinced that the combined approach herein recommended would be extremely beneficial for industrial applications. More specifically, the combination of experimental data and mechanistic models allows accurate prediction of process performance and, thus, a more robust process design. In fact, the selection of operating conditions on the basis of a limited number of empirical observations is no more sufficient, since it is associated with a too high risk of product failure. By contrast, a deeper understanding of process phenomena and the use of a more systematic approach would maximize the chances of meeting the desired product requirements. This is in line with the current emphasis on Quality by Design (QbD) [103, 104]. QbD is a concept which focuses on process control and robustness, to be achieved by deep knowledge of process behavior. The advantages of this increased process understanding would be manifold, including enhanced manufacturing efficiency, reduced risk of product failure and cost savings.

When controlled freezing approaches are used, both cooling rate and nucleation temperature may be controlled, while in the case of conventional freezing, the nucleation temperature will necessarily remain a random variable, stochastically distributed within the batch. In this last situation, to take into account this heterogeneity, freeze-drying processes should be designed for the worst-case scenarios. However, this approach may result in suboptimal process efficiency, and therefore the implementation of controlled nucleation would be highly recommended. Furthermore, it must be considered that the water removal during freeze-drying is not only by ice sublimation (primary drying) but also by vaporization from the freeze-concentrated phase (secondary drying). The freeze-concentrated phase is usually in a glassy state, whose viscous flow may cause collapse of the dried layer depending on temperature, evaporation rate and dried layer strength [105-111]. A recent study suggested that completion of the freeze-concentration process is not always achieved, especially when rapid freezing is applied [111]. In that case, removal of water from the imperfect freeze-concentrated phase would cause deformation of the original microstructures of the frozen system. To address this problem, annealing may be applied to complete freeze-concentration. During annealing, the glassy phase relaxation and Ostwald ripening would jointly modify the ice crystal morphology, and the dominant mechanism was found to depend on the stage of annealing [111].

Implementation of controlled freezing technologies in industrial plants

In recent years, because of the recognition of the determinant impact of freezing on product quality control, the interest for controlled nucleation boosted out, and almost all the principal freeze-dryers manufacturers developed their proprietary technology. Many patents were deposited, and different technical solutions were made commercially available, especially at the pilot scale. Even if many difficulties still limit the application of some methods to large production scales, controlled ice nucleation starts moving into manufacturing, as well [6, 16, 17, 112-114]. In this section a short account of current solutions and of their strengths and weaknesses will be given.

For instance, electrofreezing has strong limitations related to the salt content of the solution and it is therefore not applicable in manufacturing. By contrast, the addition of ice nucleating agents (INA) may be eventually considered for application in the food industry, but it is not of practical use for FDA-regulated and approved pharmaceutical products. In addition, it must be mentioned that despite being often used in

research, the addition of INAs does not allow control of nucleation. In fact, while the nucleation temperature is increased upon addition of nucleating agents, the problem of high batch heterogeneity is not addressed by this technique.

Ultrasound nucleation has been the object of extensive research, as discussed before, but the passage from lab to commercial scale faced strong difficulties, notwithstanding the promising results. In fact, efficient propagation of the ultrasonic waves is not easily achieved, and scaling-up of the process is not straightforward, since the optimum ultrasonic frequency depends on the system set up. As a consequence, a significant number of vials might remain non-nucleated, partly because of the possible presence of nodal points, with minimal ultrasonic intensity, on the shelf. The efficiency of nucleation may anyway be enhanced, reducing pressure or dissolving a volatile fluid in the solution [115]. In the context of an European Project, a pilot scale prototype (*LyoGamma Special* by Telstar, Spain) was realized, that allowed the testing of different technical solutions [34, 36, 37]. The positioning of the ultrasound probe below the shelf required frequent degassing of the heat transfer medium (silicon oil) and interfered with vial stoppering. Moreover, the presence of the probe made maintenance problematic. Further developments made it possible to overcome these problems, for instance by directly installing bigger transducers onto the shelves. These transducers were then activated in sequence and scanned over different wavelengths to avoid the presence of nodes in fixed locations (M. Galan, personal communication). These solutions were anyway technically complex and expensive, and hardly compatible with GMP and sterility requirements. Therefore, this line of development was set aside, and alternative methods, characterized by easier commercial implementation, became available in the meantime.

At present, commercially available equipment adopts either a variant of the ice fog technique, of the depressurization method, or the vacuum induced nucleation [116].

The ice fog concept was probably the first method to be proposed for the control of nucleation (it is known since 1990), but only recent technical developments made it suitable for practical applications [16]. The small ice crystals, formed by injecting cold nitrogen in the humid drying chamber, are obviously effective in promoting ice nucleation within the vials. Moreover, it has been shown that the ice seed are so tiny that no added water is detected in the samples after the ice fog injection [117]. However, it is necessary that these ice crystals penetrate into all the vials, and at the same time. Obviously, this task becomes

increasingly difficult as the size of the apparatus increases, and ad hoc solutions may be required to promote mixing and improve hydrodynamics inside the chamber. As a matter of fact, in the work by Rambhatla et al. the time interval for nucleation resulted very long, and, also because of the continuous cooling, the homogeneity of the batch was therefore poor [47]. Improvements were obtained by partially depressurizing the chamber (approximately to 66 mbar) and using a holed tube to distribute the ice fog. It was also suggested to use the CIP/SIP equipment already available in manufacturing freeze-dryers [48]. It became evident that the generation of a sufficiently dense ice fog and its uniform distribution represented a major issue, which may require the design of internal convection devices or other ad hoc solutions. Some concern is also related to the possible contamination by extraneous material entering the vial and, therefore, difficult compliance with the sterility requirements. Finally, a liquid nitrogen heat exchanger is used to cool the entering gas, and the use of liquid nitrogen adds complexity to the process and makes it more expensive.

In the *LyoCoN* method proposed by Martin Christ [118], the ice fog is formed in the condenser or another ice chamber, were the ice crystals are accumulated. Then, vacuum (about 10 mbar) is established in the freeze-dryer, while the condenser, or the ice chamber, are connected to an external reservoir, maintained at atmospheric pressure. As a result, when the valve between the drier and the condenser, or the ice chamber, is opened, the ice fog is transported into the drying chamber. Similarly, the *FreezeBooster*® concept by Millrock [119] utilizes the pressure differential between the product chamber and an external condenser, which works as ice seed generator, to instantly distribute the ice fog. At present, this apparatus is commercialized to retrofit lab scale or manufacturing units with a shelf surface up to about 9 m^2, but it is also being tested in pilot scale equipment up to 20 m^2 (Millrock, personal communication). Ice seeding can be coupled with control of the freezing rate to improve uniformity of the ice structure, as well [50]. Moreover, while the use of an additional external condenser allows better control of sterility, the same technique may be applied using the internal condenser [49], especially for lab-scale equipment. In this case, pressure inside the product chamber should be reduced to approximately 3.7 mbar, which resulted to be the optimum set point value, while the condenser is kept at a higher pressure. Then, the opening of the vapor port creates gas turbulence that breaks down the condensed frost into ice crystals that rapidly enter the product chamber. The original patent [119] has then been modified to improve the nucleation efficiency. For instance, in [120] it was suggested to create a predetermined volume of condensed frost on the inner surface of a condenser

connected to the product chamber and kept at a higher pressure. Afterwards, when the product chamber and the condenser are connected, the strong turbulence can knock off the frost formed on the surface of the condenser, breaking it into large ice crystals. These large crystals can last longer in the product chamber, improving the performance of the method [120]. Moreover, while in [119] the volume of the ice fog was limited by the condenser volume, in [120] the thickness of the frost can easily be controlled to achieve the desired density of ice crystals. Thus, according to the concept described in [120], the condenser volume may be reduced to increase the velocity of the gas in the condenser and the resulting turbulence. In a third version [121], a mixture of water vapor and CO_2 gas is introduced into a condenser chamber separate from the product chamber to create a predetermined volume of condensed frost, ice and dry ice crystals on an inner surface.

A modification of the technique described by Geidobler et al. [49] is said to be at the basis of the *LYOSPARK* developed by GEA [122]. Geidobler claimed that depressurization, followed by abrupt venting of the product chamber through the condenser venting valve at 3.7 mbar absolute pressure, could efficiently trigger immediate nucleation in all vials of the batch. However, a series of experiments showed early ice nucleation, prior to venting, as well as absence of ice nucleation after the venting procedure. It was therefore concluded that the value for the venting pressure theorized in [49] could not be confirmed. Moreover, to comply with the sterility requirements, it was necessary to avoid any unfiltered current from the condenser to the product chamber. Therefore, a cooling trap (with a manual valve) was mounted onto the freeze-dryer. Then, during the venting step, the cold gas from the condenser was filtered and blown through the cooling trap, where it scraped off the ice crystals stuck to the surface, carrying them into the chamber. The method is claimed to have been already tested in a pilot-scale freeze dryer (5 m^2 shelf area) as well as in a production-scale model (42 m^2 shelf area).

A further development of the ice fog technique, i. e., *VERISEQ*®, was proposed by Linde and IMA, who addressed the problem of sterility, control of the ice fog density (increasing its value to improve efficiency) and good and uniform dispersion [51, 123]. According to patents, sterile steam [124], or a humid gas [125], and liquid nitrogen (produced from sterile-filtered gaseous nitrogen in a heat exchanger) are mixed using a suitable device (an injector) outside the lyophilization chamber. The distribution of the ice fog is then improved by recirculating the ice crystals. The system has no moving parts, and both the gas velocity and the

amount of ice crystals formed can be easily controlled. This technique resulted suitable also for manufacturing scale, as success was reported in inducing nucleation for a 56 m^2 production apparatus, with more than 195,000 vials [126].

Another possible concept is based on pressurization of the chamber, followed by rapid depressurization. Scientifically known as depressurization method, it was patented by Praxair [44, 127, 128] and commercialized as *ControLyo*™. Developed and tested in cooperation with different companies, it resulted a simple and relatively scalable method [45, 129], even if the working principle is still unclear. It was initially licensed to different manufacturers (SP Scientific, GEA), and recently acquired in exclusive by SP Scientific. The system consists of a freeze-drying chamber, a gas circuit to pressurize the freeze-drying chamber, and a separate circuit for depressurization. The detailed construction of a freeze-dryer implementing this technology is described in the patent by Rampersad et al. [127]. However, it is relatively easy to retrofit a commercial freeze-dryer that has steam-in-place (SIP) capability with the manifolds and controls required for application of this technology [116]. The depressurization method is thus well suited for industrial apparatus, which can sustain pressure higher than atmospheric, while lab freeze-dryer cannot be retrofitted with this technology.

Anyway, sterilization is generally carried out at 1.2 bar relative pressure, and the apparatus is tested at 1.5 bar. Initially, quite high pressures were considered for the method. For instance, relative pressures up to 3.5 bar are reported [6], and 2 relative bar were used for example by Konstantinidis et al. [45]. Such high pressure would require an ad hoc design for industrial apparatus, as well. At present, using an appropriate gas (for example argon is better than nitrogen), the process can be carried out with an overpressure smaller than or equal to 1.5 bar. In the last version of the patent [130], it is claimed that the chamber must be pressurized to a pressure between ambient pressure and 1.7 bar. Afterwards, the pressure must be rapidly decreased (at a rate higher than 0.014 bar/s), and the pressure drop must be about 0.5 bar.

The depressurization rate is the element that may limit the applicability to large units, as it poses constrains to the geometric characteristics of the apparatus and of the depressurization circuit. Initially, application of this technology was therefore limited to pilot scale equipment (shelf surface between 1 and 5 m^2) [44, 131], but recently the retrofit of a unit up to 28 m^2 was reported [116].

The easiest and cheapest way to control nucleation is surely the vacuum induced surface freezing (VISF, also known as vacuum induced nucleation, VIN), as this technology requires no hardware, any equipment can be easily retrofitted, and there are no sterility concerns. Originally proposed by Kramer et al. [18], the method was also patented and assigned to Bayer [132], but then abandoned, mainly because of the aesthetic defects observed in the product. Actually, with some modifications (as proposed in [9, 19]), the VISF technology resulted to be extremely effective, even if the operating conditions should be accurately tuned for each product, in order to avoid the risk of boiling and puffing [133]. To this purpose, it is important to control the pressure of nucleation, as well as the temperature and holding time for the different steps involved in this technique. In addition, it is important that the amount of gas dissolved in the solution is reduced to a very low level, as escaping gases during pressure decrease are the main reason for aesthetic defects; in fact, degassing and handling of the solution is critical. In this regard, Hof Sonderanlagenbaw GmbH proposed a process modification where degassing was obtained in the freeze-dryer at elevated temperature and under partial vacuum at the same time [134]. Different temperature-pressure profiles were proposed, but this first version of what was commercially named "*SyncroFreeze*" resulted to be effective only with crystalline samples (like mannitol formulations); in case of amorphous formulations, skin formation and then collapse during ramp up to primary drying was observed [135]. It must be noted, anyway, that the boiling risk exists also for some of the ice fog concepts that were proposed, in which the chamber was depressurized down to a few Pa.

VISF is currently being developed by Azbil-Telstar (and commercialized as VIN) [20] and by HOF (*SynchroFreeze*) [123]. Its scalability is currently under evaluation: up to now it has been installed in a unit with 12 m^2 shelf surface (Azbil Telstar, personal communication) and is currently tested in a 30 m^2 industrial apparatus. The problematic is somehow similar to the depressurization method, as the control of the pressure decrease and increase rate is critical. HOF has modified the original version of *SynchroFreeze* to make it more robust including as additional process step, beside the degassing step, an increase in pressure after nucleation, together with the dosing of the closing valve [135].

Some concern exists for possible product denaturation, in particular for the depressurization and the VISF method because of the possible presence of small bubbles. In spite of this, the controlled nucleation

technologies were generally proven to improve the stability of very sensitive products like enzymes and monoclonal antibodies (17, 129, 136, 137), mainly because of the large ice crystals which are formed.

Therefore, the described methods are effective approaches to process intensification [138], but, in order to guarantee the required quality and uniformity of the product, they must be coupled with methods that assure the temperature uniformity of all the vials.

Conclusions

In the present work, we have summarized the tools which have been developed to control, measure and predict the influence of freezing conditions on product morphology, and, thus, on the freeze-drying process. These tools can be used as free-standing, self-sufficient approaches, but the best way to exploit their potential is to combine them. It is our opinion that the synergistic effects, resulting from their joint application to the design of a freeze-drying process, would be extremely beneficial.

Furthermore, the control of the nucleation temperature combined with mathematical modeling can be used to calculate the design space for both freezing and drying [138]. A design space is a graph which relates the operating conditions employed to the critical attributes of the process, defined as those properties or characteristics that should be within an appropriate range or distribution to ensure the desired product quality. Thus, it allows fast and knowledge-driven design of suitable process conditions, which guarantee process efficiency and product quality at the same time. The design space is an important tool, especially in the framework of QbD, and its use is particularly recommended in the pharmaceutical industry, where product quality and process control play a crucial role.

With the present work, we aim to stimulate the transition towards the implementation of these tools in the industrial manufacturing, as well. Considering the increasing importance given to process performance and the ever more stringent quality standards in the pharmaceutical industry, this transition would be highly desirable.

LIST OF SYMBOLS

D_{eff} effective diffusion coefficient, $m^2\ s^{-1}$

D_p pore diameter, m

ΔH_s latent heat of sublimation, $J\ kg^{-1}$

J_w mass flux, $kg\ s^{-1}\ m^{-2}$

k_v heat transfer coefficient, $W\ m^{-2}\ K^{-1}$

L path length, m

L_0 distance between the origin and the end, m

L_d dried cake thickness, m

l_{eff} effective pore length, m

M_w molar mass of water, $kg\ mol^{-1}$

n total number of pores, -

$p_{w,i}$ vapor pressure of ice, Pa

p_c chamber pressure, Pa

R universal gas constant, $J\ mol^{-1}\ K^{-1}$

R_p mass transfer resistance, $m\ s^{-1}$

T gas temperature, K

T_f temperature of the heat transfer fluid, K

T_n holding temperature at which nucleation is triggered

T_p product temperature, K

V_s volume of the solid, m^3

z axial coordinate, m

Greek letters

ε porosity, -

θ diagonal angle of the rectangular pore cross section, -

ρ_s density of the solid, $kg\ m^{-3}$

τ tortuosity, -

φ pore inclination from the vertical axis, -

Abbreviations

FDM Freeze-drying microscope

GMP Good Manufacturing Practice

INA Ice nucleating agent

QbD Quality by Design

PRT Pressure rise test

SSA specific surface area, m^2

UIIN Ultrasound induced ice nuclation

References

[1] Franks, F.; Auffret, T. Freeze-Drying of Pharmaceuticals and Biopharmaceuticals; RCS Publishing: Cambridge, UK, 2007.

[2] Rey, L.; May, J.C. Freeze-Drying/Lyophilization of Pharmaceutical and Biological Products; Taylor & Francis: New York, USA, 2010.

[3] Pikal, M.J.; Rambhatla, S.; Ramot, R. The impact of the freezing stage in lyophilization: effects of the ice nucleation temperature on process design and product quality. American Pharmaceutical Review 2002, 5 (3), 48-53.

[4] Hottot, A.; Vessot, S.; Andrieu, J. Freeze-drying of pharmaceuticals in vials: influence of freezing protocol and sample configuration on ice morphology and freeze-dried cake texture. Chemical Engineering and Processing: Process Intensification 2007, 46 (7), 666-674.

[5] Searles, J.; Carpenter, J.; Randolph, T. The ice nucleation temperature determines the primary drying rate of lyophilization for samples frozen on a temperature-controlled shelf. Journal of Pharmaceutical Sciences 2001, 90 (7), 860-871.

[6] Kasper, J.C.; Friess, W.F. The freezing step in lyophilization: Physico-chemical fundamentals, freezing methods and consequences on process performance and quality attributes of biopharmaceuticals. European Journal of Pharmaceutics and Biopharmaceutics 2011, 78 (2), 248–63.

[7] Capozzi, L.C.; Pisano, R. Looking inside the 'black box': Freezing engineering to ensure the quality of freeze-dried biopharmaceuticals. European Journal of Pharmaceutics and Biopharmaceutics 2018, 129, 58-65.

[8] Liao, X.; Krishnamurthy, R.; Suryanarayanan, R. Influence of processing conditions on the physical state of mannitol. Implications in freeze-drying. Pharmaceutical Research 2006, 24 (2), 370-376.

[9] Oddone, I.; Van Bockstal, P.-J.; De Beer, T.; Pisano, R. Impact of vacuum-induced surface freezing on inter- and intra-vial heterogeneity. European Journal of Pharmaceutics and Biopharmaceutics 2016, 103 (1), 167-178.

[10] Gorth, P. Chemical Crystallography, Part Three, Aliphatic and Aromatic Hydrocarbon Compounds; Wilhelm Engelmann: Leipzig, 1910.

[11] Williams, N.A.; Dean, T. Vial breakage by frozen mannitol solutions: Correlation with thermal characteristics and effect of stereoisomerism, additives, and vial configuration. Journal of Parenteral Science and Technology 1991, 45 (2), 94–100.

[12] Williams, N.A.; Lee, Y.; Polli, G.P.; Jennings, T.A. The effects of cooling rate on solid phase transitions and associated vial breakage occurring in frozen mannitol solutions. Journal of Parenteral Science and Technology 1986, 40 (4), 135–141.

[13] Oddone, I.; Barresi, A.A.; Pisano, R. Influence of controlled ice nucleation on the freeze-drying of pharmaceutical products: the secondary drying step. International Journal of Pharmaceutics 2017, 524 (1-2), 134-140.

[14] Fissore, D.; Pisano, R. Computer-aided framework for the design of freeze-drying cycles: Optimization of the operating conditions of the primary drying stage. Processes 2015, 3(2), 406-421.

[15] Bhatnagar, B.S.; Pikal, M.J.; Robin, H.B. Study of the individual contributions of ice formation and freeze-concentration on isothermal stability of lactate dehydrogenase during freezing. Journal of Pharmaceutical Sciences 2008, 97 (2), 798-814.

[16] Geidobler, R.; Winter, G. Controlled ice nucleation in the field of freeze-drying: fundamentals and technology review. European Journal of Pharmaceutics and Biopharmaceutics 2013, 85 (2), 214-222.

[17] Pisano, R. Alternative methods of controlling nucleation in freeze-drying. In Lyophilization of Pharmaceuticals, Vaccines, and Medical Diagnostics; Ward, K.R., Matejtschuk, P., Eds.; Springer: New York, *in press*.

[18] Kramer, M.; Sennhenn, B.; Lee, G. Freeze-drying using vacuum-induced surface freezing. Journal of Pharmaceutical Sciences 2002, 91 (2), 433-443.

[19] Liu, J.; Viverette, T.; Virgin, M.; Anderson, M.; Dalal, P. A study of the impact of freezing on the lyophilization of a concentrated formulation with a high fill depth. Pharmaceutical Development and Technology 2005, 10 (2), 261-272.

[20] Oddone, I.; Pisano, R.; Bullich, R.; Stewart, P. Vacuum-induced nucleation as a method for freeze-drying cycle optimization. Industrial & Engineering Chemistry Research 2014, 53 (47), 18236-18244.

[21] Hunt, J.D.; Jackson, K.A. Nucleation of solid in an undercooled liquid by cavitation. Journal of Applied Physics 1966, 37 (1), 254-257.

[22] Zhang, X.; Inada, T.; Yabe, A.; Lu, S.; Kozawa, Y. Active control of phase change from supercooled water to ice by ultrasonic vibration, Part 2: Generation of ice slurries and effect of bubble nuclei. International Journal of Heat and Mass Transfer 2001, 44 (23), 4533-4539.
[23] Zhang, X.; Inada, T.; Tezuka, A. Ultrasonic-induced nucleation of ice in water containing air bubbles. Ultrasonics Sonochemistry 2003, 10 (2), 71-76.
[24] Pilli, S.; Bhunia, P.; Yan, S.; LeBlanc, R.J.; Tyagi, R.D. Ultrasonic pretreament of sludge: A review. Ultrasonics Sonochemistry 2011, 18 (1), 1-18.
[25] Rastogi, N.K. Opportunities and challenges in application of ultrasound in food processing. Critical Reviews in Food Science and Nutrition 2011, 51 (8), 705-722.
[26] Hickling, R. Nucleation of freezing by cavity collapse and its relation to cavitation damage. Nature 1965, 206 (4987): 915-917.
[27] Saclier, M.; Peczalski, R.; Andrieu, J. A theoretical model for ice primary nucleation induced by acoustic cavitation. Ultrasonics Sonochemistry 2010, 17 (1), 98-105.
[28] Ohsaka, K.; Trinh, E.H. Dynamic nucleation of ice induced by a single stable cavitation bubble. Applied Physics Letters 1998, 73 (129), 129-31.
[29] Hozumi, T.; Saito, A.; Okawa, S.; Matsui, T. Freezing phenomena of supercooled water under impacts of ultrasonic waves. International Journal of Refrigeration 2002, 25(7), 948-53.
[30] Inada, T.; Zhang, X.; Yabe, A.; Kozawa, Y. Active control of phase change from supercooled water to ice by ultrasonic vibration, Part 1: Control of freezing temperature. International Journal of Heat and Mass Transfer 2001, 44 (23), 4523-4531.
[31] Chow R.; Blindt R.; Chivers, R.; Povey M., The sonocrystallisation of ice in sucrose solutions: Primary and secondary nucleation. Ultrasonics 2003, 41 (8), 595-604.
[32] Nakagawa, K.; Hottot, A.; Vessot, S.; Andrieu, J. Influence of controlled nucleation by ultrasounds on ice morphology of frozen formulations for pharmaceutical proteins freeze-drying. Chemical Engineering and Processing: Process Intensification 2006, 45 (9), 783-791.
[33] Hottot, A.; Nakagawa, K.; Andrieu, J. Effect of ultrasound-controlled nucleation on structural and morphological properties of freeze-dried mannitol solutions. Chemical Engineering Research and Design 2008, 86 (2), 193-200.
[34] Passot, S.; Trelea, I.C.; Marin, M.; Galan, M.; Morris, G.J.; Fonseca, F. Effect of controlled ice nucleation on primary drying stage and protein recovery in vials cooled in a modified freeze-dryer. Journal of Biomechanical Engineering 2009, 131 (7), 074511.
[35] Nakagawa, K.; Hottot, A.; Vessot, A.; Andrieu, J. Modeling of freezing step during freeze-drying of drugs in vials. AIChE Journal 2007, 53 (5), 1362-1372.
[36] Morris, J.; Morris, G.J.; Taylor, R.; Zhai, S.; Slater, N.K.H. The effect of controlled nucleation of ice on the ice structure, drying rate, and protein recovery in vials cooled in modified shelf freeze drier. In Abstracts of papers and posters presented at the Forty-First Annual Meeting of the Society for Cryobiology in association with the Japanese Societies & Associations for Cryobiology, Cryopreservation and Cryomedicine, and the Chinese Cryobiology Society (#48). Cryobiology 2004, 49, 308-309.
[37] Fissore, D.; Barresi, A.A. In-line product quality control of pharmaceuticals in freeze-drying processes. In Modern Drying Technology Vol. 3: Product Quality and Formulation; Tsotsas, E., Mujumdar, A.S., Eds.; Wiley-VCH Verlag GmbH & Co. KGaA: Weinhein, 2011; Chap. 4, 91-154.
[38] Arends, B.J.; Blindt, R.A.; Janssen, J.; Patrick, M. Crystallisation process using ultrasound. Patent US 6630185 B2, Occtober 7, 2003. Patent EP 1409100 B1, December 30, 2009.
[39] Rau, W. Eiskeimbildung durch Dielektrische Polarisation. Zeitschrift für Naturforschung A 1951, 6 (11), 649-657.
[40] Petersen, A.; Schneider, H.; Rau, G.; Glasmacher, B. A new approach for freezing of aqueous solutions under active control of the nucleation temperature. Criobiology 2006, 53 (2), 248-257.
[41] Margaritis, A.; Bassi, A.S. Principles and biotechnological applications of bacterial ice nucleation. Critical Reviews in Biotechnology 1991, 11 (3), 277-295.
[42] Cochet, N.; Widehem, P. Ice crystallization by *Pseudomonas syringae*. Applied Microbiology and Biotechnology 2000, 54(2), 153-161.
[43] Lindong, W.; Shannon, N.; Anisa, S.; Shannon, L.; Mehmet, T. Controlled ice nucleation using freeze-dried *Pseudomonas syringae* encapsulated in alginate beads. Cryobiology 2017, 75 (4), 1-6.
[44] Bursac, R.; Sever, R.; Hunek, B. A practical method for resolving the nucleation problem in lyophilization. BioProcess International 2009, 7 (9), 6672.

[45] Konstantinidis, A.K.; Kuu, W.; Otten, L.; Nail, S.L.; Sever, R.R.; Bons, V.; Debo, D.; Pikal, M.J. Controlled nucleation in freeze-drying: Effects on pore size in the dried product layer, mass transfer resistance, and primary drying rate. Journal of Pharmaceutical Sciences 2011, 100 (8), 3453-3470.
[46] Rowe, T.W. A technique for the nucleation of ice. In Proceedings of International Symposium on Biological Product Freeze-Drying and Formulation, Bethesda, USA, October 24-26, 1990. Development in Biological Standardization 1992, 74, 377.
[47] Rambhatla, S.; Ramot, R.; Bhugra, C.; Pikal, M.J. Heat and mass transfer scale-up issues during freeze drying: II. Control and characterization of the degree of supercooling. AAPS PharmSciTech 2004, 5 (4), 54-62.
[48] Patel, S.M.; Bhugra, C.; Pikal, M.J. Reduced pressure ice fog technique for controlled ice nucleation during freeze-drying. AAPS PharmSciTech 2009, 10 (4), 1406-1411.
[49] Geidobler, R.; Mannschedel, S.; Winter, G. A new approach to achieve controlled ice nucleation of supercooled solutions during the freezing step in freeze-drying. Journal of Pharmaceutical Sciences 2012, 101 (12), 4409-4413.
[50] Thompson, T.N. Lyopat^{TM}: Real-time monitoring and control of the freezing and primary drying stages during freeze-drying for improved product quality and reduced cycle times. American Pharmaceutical Review 2013, 16 (7), 625. Available at http://www.americanpharmaceuticalreview.com.
[51] Chakravarty, P.; Lee, R.; Demarco, F.; Renzi, E. Ice fog as a means to induce uniform ice nucleation during lyophilization. Biopharm International 2012, 25 (1), 33-38.
[52] Kharaghani, A.; Tsotsas, E.; Wolf, C.; Beutler, T.; Guttzeit, M.; Oetjen, G.-W. Freeze-Drying. In Ullmann's Encyclopedia of Industrial Chemistry, (Ed.). doi:10.1002/14356007.h12_h01.pub2
[53] Pisano, R.; Fissore, D.; Barresi, A.A. Freeze-drying cycle optimization using model predictive control techniques. Industrial and Engineering Chemistry Research 2011, 50 (12), 7363-7379
[54] Hottot, A.; Vessot, S.; Andrieu, J. Determination of mass and heat transfer parameters during freeze-drying cycles of pharmaceutical products. PDA Journal of Pharmaceutical Science and Technology 2005, 59 (2), 138-153.
[55] Kuu, W.Y.; Hardwick, L.M.; Akers, M.J. Rapid determination of dry layer resistance to various pharmaceutical formulations during primary drying using product temperature profiles. International Journal of Pharmaceutics 2006, 313 (1), 99-113.
[56] Kuu, W.Y.; Obryan, K.R.; Hardwick, L.M.; Paul, T.W. Product mass transfer resistance directly determined during freeze-drying cycle runs using tunable diode laser absorption spectroscopy (TDLAS) and pore diffusion model. Pharmaceutical Development and Technology 2011, 16 (4), 343-357.
[57] Kodama, T.; Sawada, H.; Hosomi, H.; Takeuchi, M.; Wakiyama, N.; Yonemochi, E.; Terada, K. Determination for dry layer resistance of sucrose under various primary drying conditions using a novel simulation program for designing pharmaceutical lyophilization cycle. International Journal of Pharmaceutics 2013, 452 (1-2), 180-187.
[58] Bosca, S.; Barresi, A.A.; Fissore, D. Use of a soft-sensor for the fast estimation of dried cake resistance during a freeze-drying cycle. International Journal of Pharmaceutics 2013, 451, 23-33.
[59] Goff, J.A.; Gratch, S. Low-pressure properties of water from -160 to 212 F. Transactions of the American Society of Heating and Ventilating Engineers 1946, 95-122. Presented at the 52nd Annual Meeting of the American Society of Heating and Ventilating Engineers, New York, 1946.
[60] Fissore, D.; Pisano, R.; Barresi, A.A. Model-based framework for the analysis of failure consequences in a freeze-drying process. Industrial & Engineering Chemistry Research 2012, 51 (38), 12386-12397.
[61] Neumann, K.H. Freeze-drying apparatus. Patent US 2994132, August 1, 1961.
[62] Milton, N.; Pikal, M.J.; Roy, M.L.; Nail, S.L. Evaluation of manometric temperature measurement as a method of monitoring product temperature during lyophilization. PDA Journal of Pharmaceutical Science & Technology 1997, 51 (1), 7-16.
[63] Pikal, M.J.; Tang, X.; Nail, S.L. Automated process control using manometric temperature measurement. Patent US 6971187 B1, December 6, 2005.
[64] Tang, X.C.; Nail, S.L.; Pikal, M.J. Freeze-drying process design by manometric temperature measurement: Design of a smart freeze-dryer. Pharmaceutical Research 2005, 22 (4), 685-700.
[65] Chouvenc, P.; Vessot, S.; Andrieu, J.; Vacus, P. Optimization of the freeze-drying cycle: A new model for pressure rise analysis. Drying Technology 2004, 22 (7), 1577-1601.
[66] Velardi, S.A.; Rasetto, V.; Barresi, A.A. Dynamic Parameters Estimation Method: Advanced Manometric Temperature Measurement approach for freeze-drying monitoring of pharmaceutical. Industrial & Engineering Chemistry Research 2008, 47 (21), 8445-8457.

[67] Velardi, S.A.; Barresi, A.A. Method and system for controlling a freeze drying process. Patent EP 2156124 B1, April 25, 2012. Patent US8800162 B2, August 12, 2014.
[68] Fissore, D.; Pisano, R.; Barresi, A.A. On the methods based on the pressure rise test for monitoring a freeze-drying process. Drying Technology 2011, 29 (1), 73-90.
[69] Barresi, A.A.; Pisano, R.; Rasetto, V.; Fissore, D.; Marchisio, D.L. Model-based monitoting and control of industrial freeze-drying processes: Effect of batch non-uniformity. Drying Technology 2010, 28 (5), 577-590.
[70] Fissore, D.; Pisano, R.; Barresi, A.A. Monitoring of the secondary drying in freeze-drying of pharmaceuticals. Journal of Pharmaceutical Sciences 2011, 100 (2), 732-742.
[71] Grassini, S.; Pisano, R.; Barresi, A.A.; Angelini, E.; Parvis, M. Frequency domain image analysis for the characterization of porous products. Measurement 2016, 94, 515-522.
[72] Parvis, M.; Grassini, S.; Angelini, E.; Pisano, R.; Barresi, A.A. Characterization of freeze-dried pharmaceutical product structures by an FFT-imaging approach. In Proceedings of IEEE International Symposium on Medical Measurements and Applications "MeMeA 2014", Lisbon, Portugal, June 11-12, 2014; 302-307.
[73] Grassini, S.; Angelini, E.; Pisano, R.; Barresi, A.; Parvis, M. Wavelet image decomposition for characterization of freeze-dried pharmaceutical product structures. In Proceedings of IEEE International Instrumentation and Measurements Technology Conference "I2MTC 2015", Pisa, Italy, May 11-14, 2015; 2072-2077.
[74] Arsiccio, A.; Sparavigna, A.C.; Pisano, R.; Barresi, A.A. Measuring and predicting pore size distribution of freeze-dried solutions. Drying Technology, *in press*. DOI: 10.1080/07373937.2018.1430042.
[75] Pisano, R.; Barresi, A.A.; Capozzi, L.C.; Novajra, G.; Oddone, I.; Vitale-Brovarone, C. Characterization of the mass transfer of lyophilized products based on X-ray micro-computed tomography images. Drying Technology 2017, 35 (8), 933-938.
[76] Liapis, A.I.; Bruttini, R. A theory for the primary and secondary drying stages of the freeze-drying of pharmaceutical crystalline and amorphous solutes: Comparison between experimental data and theory. Separation Technology 1994, 4 (3), 144-155.
[77] Comiti, J.; Renaud, M. A new model for determining mean structure parameters of fixed beds from pressure drop measurements: application to beds packed with parallelepipedal particles. Chemical Engineering Science 1989, 44 (7), 1539-1545.
[78] Warning, A.; Verboven, P.; Nicolaï, B.; van Dalen, G.; Datta, A.K. Computation of mass transport properties of apple and rice from X-ray microtomography images. Innovative Food Science & Emerging Technologies 2014, 24, 14-27.
[79] Li, S.; Stawczyk, J.; Zbicinski, I. CFD model of apple atmospheric freeze drying at low temperature. Drying Technology 2007, 25 (7-8), 1331-1339.
[80] Nakagawa, K.; Ochiai, T. A mathematical model of multi-dimensional freeze-drying for food products. Journal of Food Engineering 2015, 161, 55-67.
[81] Goshima, H.; Do, G.; Nakagawa, K. Impact of ice morphology on design space of pharmaceutical freeze-drying. Journal of Pharmaceutical Sciences 2016, 105 (6), 1920-1933.
[82] Capozzi, L.C.; Arsiccio, A.; Sparavigna, A.C.; Pisano, R.; Barresi, A.A. Image segmentation and 3D reconstruction for improved prediction of the sublimation rate during freeze drying. In Proceedings of *21st International Drying Symposium IDS'2018*, Valencia, Spain, September 11-14, 2018; paper 7646.
[83] Raman, P. 2015. Freeze drying microscopy as a tool to study sublimation kinetics, PhD. Thesis, Loughborough University, UK; available at https://dspace.lboro.ac.uk/2134/18316.
[84] Ray, P.; Rielly, C.D.; Stapley, A.G.F. A freeze-drying microscopy study of the kinetics of sublimation in a model lactose system. Chemical Engineering Science 2017, 172, 731-743.
[85] Kochs, M.; Schwindke, P.; Körber, C. A microscope stage for the dynamic observation of freezing and freeze-drying in solutions and cell-suspensions. Cryo-Letters 1989, 10, 401-420.
[86] Pikal, M.J.; Shah, S.; Senior, D.; Lang, J.E.. Physical-chemistry of freeze-drying – measurement of sublimation rates for frozen aqueous solutions by a microbalance technique. Journal of Pharmaceutical Sciences 1983, 72, 635-650.
[87] Kochs, M.; Korber, C.; Nunner, B.; Heschel, I. The influence of the freezing process on vapor transport during sublimation in vacuum-freeze-drying. International Journal of Heat and Mass Transfer 1991, 34, 2395-2408.

[88] Zhai, S.; Taylor, R.; Sanches, R.; Slater, N.K.H. Measurement of lyophilisation primary drying rates by freeze-drying microscopy. Chemical Engineering Science 2003, 58 (11), 2313-2323.
[89] Meister, E.; Gieseler, H. Freeze-dry microscopy of protein/sugar mixtures: Drying behaviour, interpretation of collapse temperature and a comparison to corresponding glass transition data. Journal of Pharmaceutical Sciences 2009, 98, 2087-3072.
[90] Nakagawa, K.; Hottot, A.; Vessot, S.; Andrieu, J. Modeling of freezing step during freeze-drying of drugs in vials. AIChE Journal 2007, 53 (5), 1362-1372.
[91] Pisano, R.; Capozzi, L. Prediction of product morphology of lyophilized drugs in the case of Vacuum Induced Surface freezing. Chemical Engineering Research & Design 2017, 125, 119-129.
[92] Bomben, J.L.; King, C.J. Heat and mass transport in the freezing of apple tissue. International Journal of Food Science & Technology 1982, 17 (5), 615-632.
[93] Kochs, M.; Korber, C.H.; Heschel, I.; Nunner, B. The influence of the freezing process on vapour transport during sublimation in vacuum freeze-drying. International Journal of Heat and Mass Transfer 1991, 34 (9), 2395-2408.
[94] Kurz, W.; Fisher, D.J. Fundamentals of Solidification; Trans Tech Publications: Switzerland, 1992.
[95] Arsiccio, A.; Barresi, A.A.; Pisano, R. Prediction of ice crystal size distribution after freezing of pharmaceutical solutions. Crystal Growth and Design 2017, 17 (9), 4573-4581.
[96] Arsiccio, A.; Pisano, R. Application of the Quality by Design approach to the freezing step of freeze-drying: Building the design space. Journal of Pharmaceutical Sciences 2018, 107 (6), 1586-1596.
[97] Xiong, Q.; Baychev, T.G.; Jivkov, A.P. Review of pore network modelling of porous media: Experimental characterisations, network constructions and applications to reactive transport. Journal of Contaminant Hydrology 2016, 192, 101-117.
[98] Blunt, M.J. Flow in porous media – pore-network models and multiphase flow. Current Opinion in Colloid and Interface Science 2001, 6 (3), 197-207.
[99] Vorhauer, N.; Tran, Q.T.; Metzger, T.; Tsotsas, E.; Prat, M. Experimental investigation of drying in a model porous medium: Influence of thermal gradients. Drying Technology 2013, 31 (8), 920-929.
[100] Prat, M. Recent advances in pore-scale models for drying of porous media. Chemical Engineering Journal 2002, 86 (1-2), 153-164.
[101] Metzger, T.; Irawan, A.; Tsotsas, E. Isothermal drying of pore networks: Influence of friction for different pore structures. Drying Technology 2007, 25 (1-3), 49-57.
[102] Kharaghani, A.; Metzger, T.; Tsotsas, E. A proposal for discrete modelling of mechanical effects during drying, combining pore network with DEM. AIChE Journal 2011, 57 (4), 872-885.
[103] Yu, L.X. Pharmaceutical Quality by Design: Product and process development, understanding, and control. Pharmaceutical Research 2008, 25 (4), 781-791.
[104] Yu, L.X.; Amidon, G.; Khan, M.A.; Hoag, S.W.; Polli, J.; Raju, G.K.; Woodcock, J. Understanding pharmaceutical Quality by Design. The AAPS Journal 2014, 16 (4), 771-783.
[105] To, E.C.; Flink, J.M. Collapse, a structural transition in freeze dried carbohydrates. III Prerequisite of recrystallization. International Journal of Food Science and Technology 1978, 13 (6), 583-594.
[106] Pikal, M.J.; Shah, S. The collapse temperature in freeze drying: Dependence on measurement methodology and rate of water removal from the glassy phase. International Journal of Pharmaceutics 1990, 62 (2-3), 165-186.
[107] Slade, L.; Levine, H.; Reid, D.S. Beyond water activity: Recent advances based on an alternative approach to the assessment of food quality and safety. Critical Reviews in Food Science and Nutrition 1991, 30 (2-3), 115-360.
[108] Levi, G.; Karel, M. Volumetric shrinkage (collapse) in freeze-dried carbohydrates above their glass transition temperature. Food Research International 1995, 28 (2), 145-151.
[109] Carpenter, J.F.; Pikal, M.J.; Chang, B.S.; Randolph, T.W. Rational design of stable lyophilized protein formulations: Some practical advice. Pharmaceutical Research 1997, 14 (8), 969-975.
[110] Meister, E.; Gieseler, H. Freeze-dry microscopy of protein/sugar mixtures: Drying behavior, interpretation of collapse temperatures and a comparison to corresponding glass transition data. Journal of Pharmaceutical Sciences 2009, 98 (9), 3072-3087.
[111] Nakagawa, S.; Tamiya, K.; Do, G.; Kono, S.; Ochiai, T. Observation of glassy state relaxation during annealing of frozen sugar solutions by X-ray computed tomography. European Journal of Pharmaceutics and Biopharmaceutics 2018, 127, 279-287.

[112] Gieseler, H.; Stärtzel, P. Controlled nucleation in freeze-drying. European Pharmaceutical Review 2012, 17 (5), https://www.europeanpharmaceuticalreview.com/article/15427/controlled-nucleation-in-freeze-drying/
[113] Anuj, G. Short review on controlled nucleation. International Journal of Drug Development & Research, 2012, 4 (3), 35-40.
[114] Thomas, P. Controlled ice nucleation moves into manufacturing. Pharmaceutical Manufacturing 2011, article 20, https://www.pharmamanufacturing.com/articles/2011/020/
[115] Acton, E.; Morris, G.J. Method and apparatus for freeze drying material. Patent Application GB 2400901 A, October 27, 2004.
[116] Siew, A. Controlling ice nucleation during the freezing step of lyophilization. Pharmaceutical Technology 2013, 37 (5), 36-40.
[117] Kodama, T; Alexeenko, A. Effect of ice fog-controlled ice nucleation on solution weight. LyoHub presentation, 2018. https://www.millrocktech.com/lyosight/lyobrary/white-papers-posters-presentations/
[118] Umbach, M. Freeze drying plant. Patent EP 3093597 B1, December 27, 2017.
[119] Ling, W. Controlled nucleation during freezing step of freeze drying cycle using pressure differential ice fog distribution. Patent US 8839528 B2, September 23, 2014. Patent EP 2702342 B1, April 20, 2014.
[120] Ling, W. Controlled nucleation during freezing step of freeze drying cycle using pressure differential ice crystals distribution from condensed frost. Patent US 8875413 B2, November 4, 2014.
[121] Ling, W. Controlled nucleation during freezing step of freeze drying cycle using pressure differential water vapor CO_2 ice crystals. Patent US 9470453 B2, October 18, 2016.
[122] GEA. Inducing nucleation in industrial freeze dryers. Manufacturing Chemist 2017 (22 Nov.). Available at https://www.manufacturingchemist.com/news/article_page/Inducing_nucleation_in_industrial_freeze_dryers/136511
[123] Brower, J.; Lee, R.; Wexler, E.; Finley, S.; Caldwell, M.; Studer, P. New developments in controlled nucleation: Commercializing VERISEQ® nucleation technology. In Lyophilized Biologics and Vaccines; Varshney, D., Singh, M., Eds.; Springer: New York (NY), 2015; 73-90.
[124] Chakravarty, P.; Lee, R.C. Method for freeze drying. Patent US 8549768 B2, October 8, 2013. Method for freeze drying and corresponding freeze dryer. Patent EP 2498035 B1, July 26, 2017.
[125] Lee, R.C.; Chakravarty, P. Freeze drying method. Patent EP 2478313 B1, October 25, 2013. Freeze drying system. Patent Application US 20110179667 A1, July 28, 2011.
[126] Azzarella, J.; Mudhivarthi, V.K.; Wexler, E.; Ganguly, A. Increasing vial to vial homogeneity: An analysis of VERISEQ® nucleation on production scale freeze dryers. BioPharm International 2017, 29 (12), 36-41, 55.
[127] Rampersad, B.M.; Sever, R.R.; Humek, B.; Gasteyer, T.H. III. Freeze-dryer and method of controlling the same. Patent US 8240065 B2, August 14, 2012.
[128] Gasteyer, T.H. III; Sever, R.R.; Hunek, B.; Grinter, N.; Verdone, M.L. Method of inducing nucleation of a material. Patent US 9453675 B2, September 25, 2016. Patent EP 1982133 B1, July 15, 2015.
[129] Awotwe-Otoo, D.; Agarabi, C.; Read, E.K.; Lute, S.; Brorson, K.A; Khan, M.A.; Shah, R.B. Impact of controlled ice nucleation on process performance and quality attributes of a lyophilized monoclonal antibody. International Journal of Pharmaceutics 2013, 450 (1-2), 70-78.
[130] Gasteyer, T.H. III; Sever, R.R.; Hunek, B.; Grinter, N.; Verdone, M.L. Lyophilization system and method. Patent US 9651305 B2, May 16, 2017. Lyophilization method, Patent EP 1982132 B1, August 10, 2016.
[131] Shon, M.; Mather, L. The importance of controlling nucleation temperature during the freeze step. Introduction of ControLyo™ nucleation on-demand technology on the New FTS/SP Scientific™ LyoStar™3 Freeze Dryer. https://www.labrepco.com/data/userfiles/files/The-Importance-of-Controlling-Nucleation-Temperature.pdf. Accessed January 2018.
[132] Sennhenn, B; Kramer, M. Lyophilization method. Patent US 6684524 B1, February 3, 2004.
[133] Arsiccio, A.; Barresi, A.A.; De Beer, T.; Oddone, I.;Van Bockstal, P.-J.; Pisano, R. Vacuum induced surface freezing as an effective method for improved inter- and intra-vial product homogeneity. European Journal of Pharmaceutics and Biopharmaceutics 2018, 128, 210-219.
[134] Hof, H.-G.; Schilder, G. Method for freeze drying a moist product which is provided with a solvent. Patent Application EP 2728287 A3, October 19, 2016.

[135] Allmendinger, A.; Schilder, G.; Mietzner, R.; Butt Y.L.; Lümkermann, J.; Lema Martinez, C. Controlled nucleation during freeze drying using vacuum-induced surface freezing. Research Disclosure 2016 (Jan), data base no. 633018, http://www.researchdisclosure.com.

[136] Wexler, E.; Brower, J. New developments in controlled nucleation. Pharmaceutical Manufacturing, 2015 (Oct 16), 26-29. https://www.pharmamanufacturing.com/articles/2015/new-developments-in-controlled-nucleation/

[137] Fang, R.; Tanaka, K.; Mudhivarthi, V.; Bogner, R.H.; Pikal, M.J. Effect of controlled ice nucleation on stability of lactate dehydrogenase during freeze-drying. Journal of Pharmaceutical Sciences 2018, 107(3), 824-830.

[138] Pisano, R.; Fissore, D.; Barresi, A.A. 2014, Intensification of freeze-drying for the pharmaceutical and food industry. In Modern Drying Technology Vol. 5: Process Intensification; Tsotsas, E., Mujumdar, A.S., Eds.; Wiley-VCH Verlag GmbH & Co. KGaA: Weinhein; Chap. 5, 131-161.

Table 1: Scheme of the effect of cooling rate and nucleation temperature on pore size and process performance.

Nucl. Temp.	Cooling Rate	Pore Size	Subl. Rate	Desorp. Rate
High	Low	Large	High	Low
Low	High	Small	Low	High

Note: If the nucleation temperature is high and/or the cooling rate is low, a large pore size will be obtained, speeding up the sublimation rate and lowering the desorption rate. By contrast, low nucleation temperature and/or high cooling rate will result in small pore size, and, therefore, decreased sublimation rate and enhanced desorption rate.

Figure Legends

Fig. 1: Primary drying time and maximum temperature reached within the product as a function of the pore size, defined as the average diameter that, introduced into Equation 1, leads to the experimental value of mass transfer resistance. The Figure was obtained by means of the model described in [13], for the case of mannitol 5% w/w and primary drying performed at 263 K and 10 Pa.

Fig. 2: a) Scheme of the Ultrasound-Induced Ice Nucleation technique. Batches of vials on different shelves of a freeze dryer are exposed to ultrasounds to promote nucleation. b) Temperature and pressure profiles during Vacuum Induced Surface Freezing.

Fig. 3: Images of freeze dried mannitol (section at top, center, and bottom of the product), in the case of a) uncontrolled freezing, b) VISF AT T_n =–5 °C and (c) UIIN at T_n=–7 °C. a) and b) are SEM images of the pores after freeze-drying while c) are optical microscopy images of the frozen samples. T_n is the holding temperature at which nucleation is triggered.

Fig. 4: Cross sectional shapes of ice crystals; the minimum pore dimension in the transversal section can be approximately taken as D_p, while l_{eff} is the mean effective length of the pore (only sections where major/minor pore length >2 were taken into consideration, and an average value over all the measured crystals was taken as representative of the analyzed sample for the model).
Right hand side figure shows, for an ideal cylindrical pore, the relationship between different geometric variables used to calculate tortuosity according to Eq. (5)–(7), depending on the original ice orientation. Adapted from [70] with permission from Elsevier.

Fig. 5: Comparison between detailed model predictions [92] (–▲–), simplified model predictions [92] (- -■ - -) and empirical laws described in: Bomben and King [89] (─△─), Kochs et al. [90] (─□─), and Kurz and Fischer [91] (- -○- -, ─◇─), for mannitol 5% w/w, in the case of (top) uncontrolled freezing and (bottom) VISF (setting the nucleation temperature to –5 °C). Experimental data, obtained from SEM observations, are reported in the box plots. Reprinted with permission from [92]. Copyright 2017, American Chemical Society.

Fig. 6: Scheme outlining the possible process for the design of optimal freezing conditions, as described in this work.

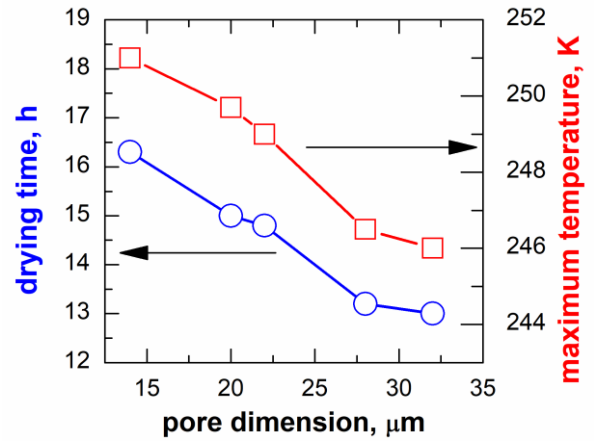
drying time, h
maximum temperature, K
pore dimension, μm
19
18
17
16
15
14
13
12
252
250
248
246
244
15
20
25
30
35

Fig. 1

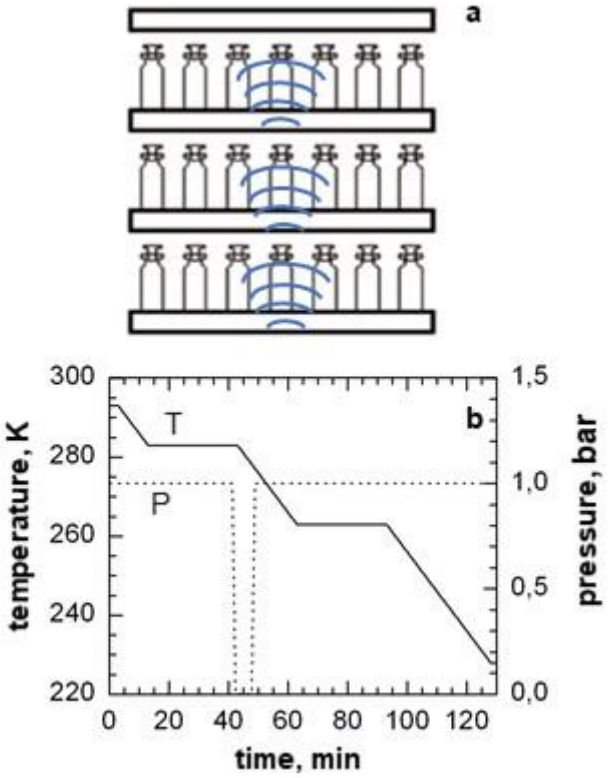
a
b
T
P
temperature, K
pressure, bar
time, min
300
280
260
240
220
1,5
1,0
0,5
0,0
0
20
40
60
80
100
120

Fig. 2

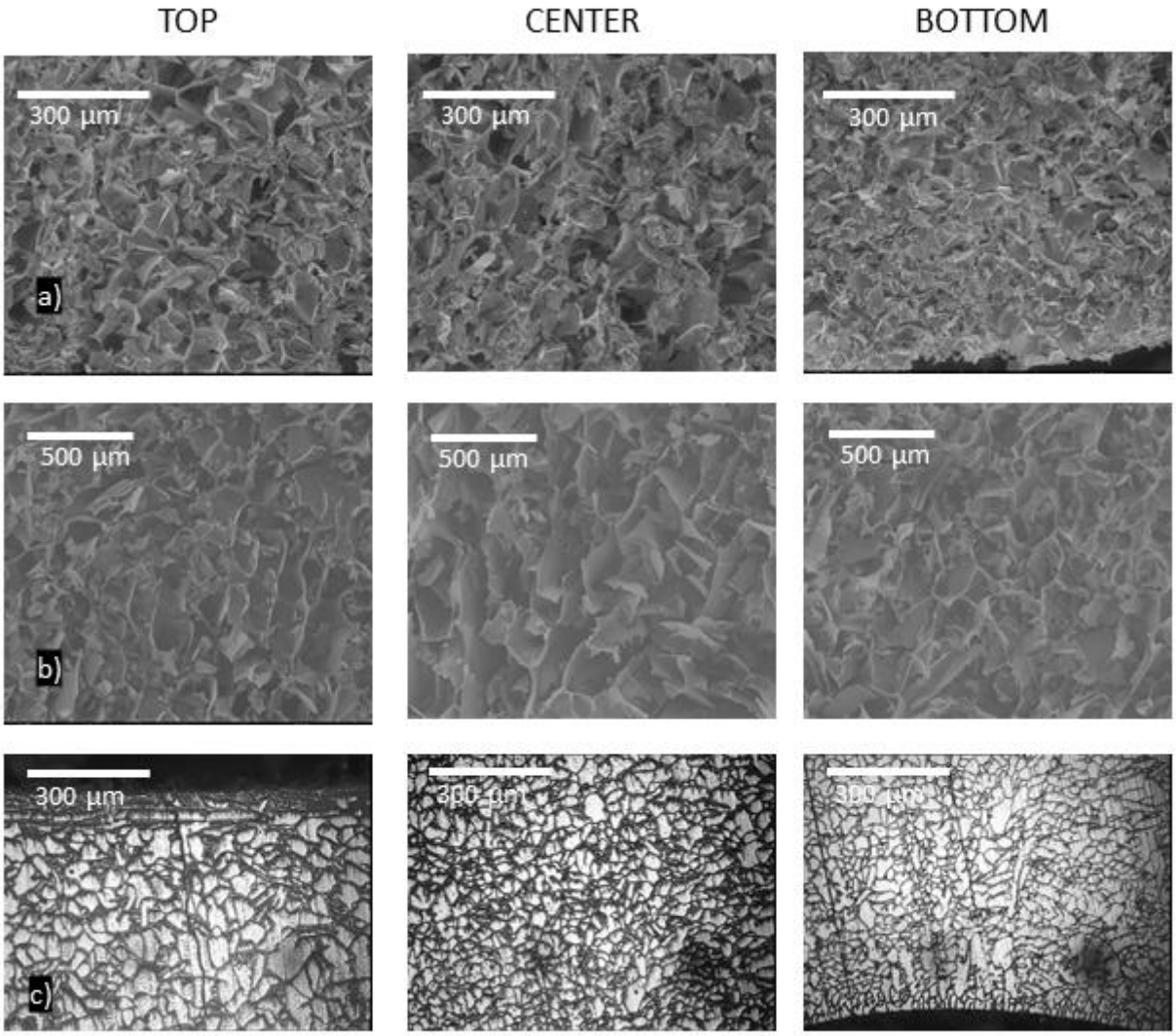
TOP
CENTER
BOTTOM
300 µm
a)
300 µm
300 µm
500 µm
b)
500 µm
500 µm
300 µm
c)
300 µm

Fig. 3

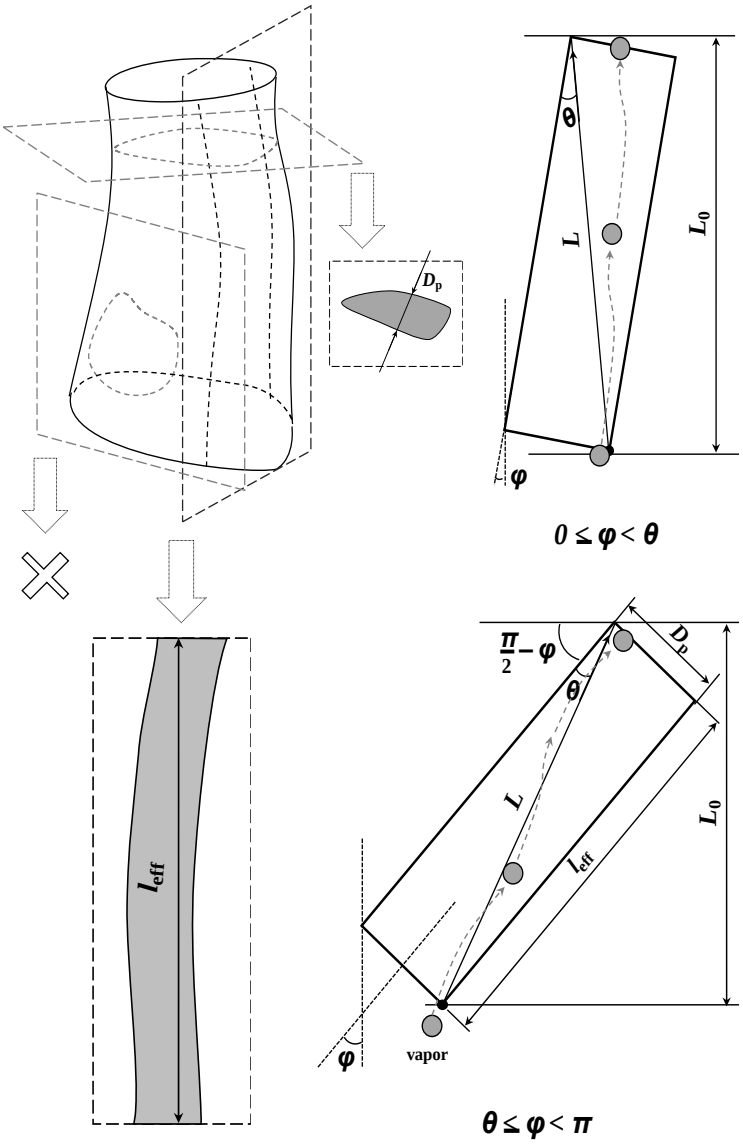
θ
L
L_0
D_p
φ
$0 \le \varphi < \theta$
$\frac{\pi}{2} - \varphi$
θ
D_p
L
L_0
l_{eff}
l_{eff}
φ
vapor
$\theta \le \varphi < \pi$

Fig. 4

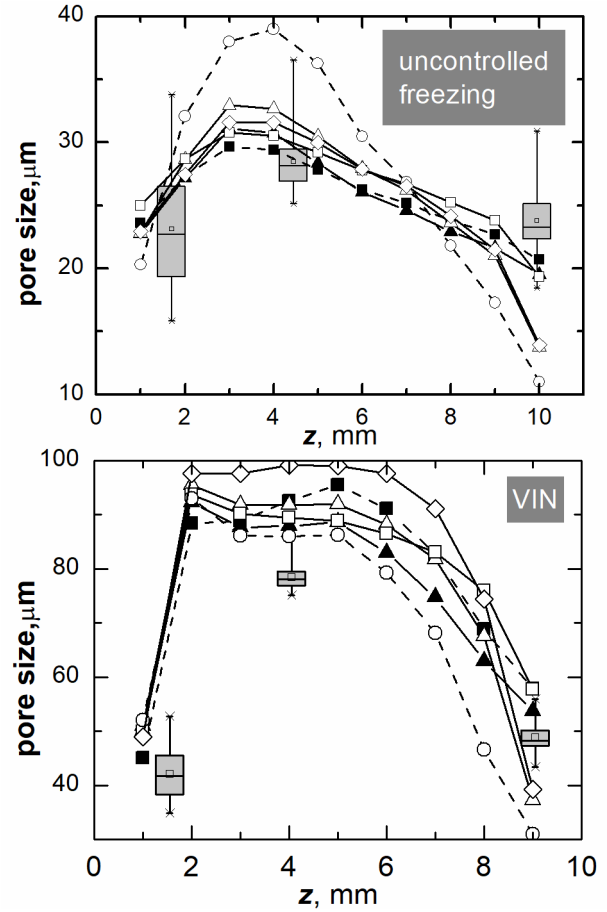

Fig. 5

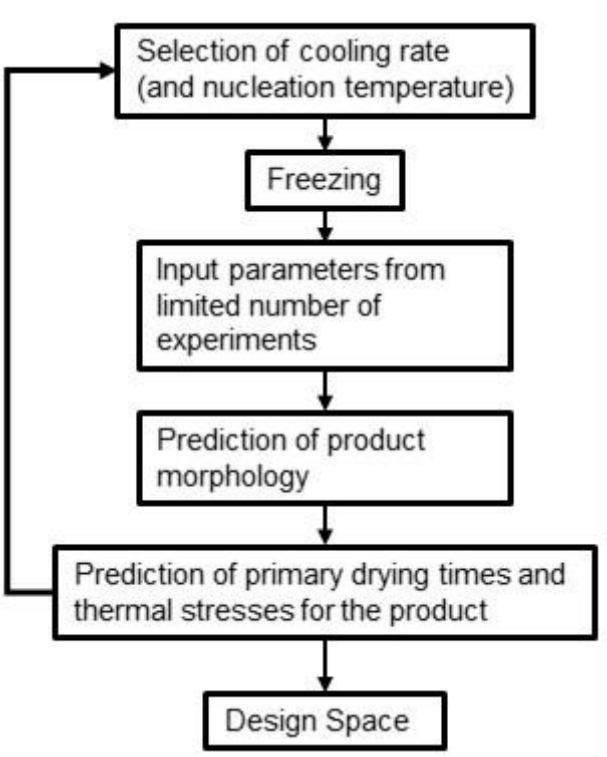
Selection of cooling rate
(and nucleation temperature)
Freezing
Input parameters from
limited number of
experiments
Prediction of product
morphology
Prediction of primary drying times and
thermal stresses for the product
Design Space

Fig. 6